Tuning Photoinduced Intramolecular Electron Transfer by Electron Accepting and Donating Substituents in Oxazolones

J Fluoresc
DOI 10.1007/s10895-013-1198-6

ORIGINAL PAPER

Tuning Photoinduced Intramolecular Electron Transfer by Electron Accepting and Donating Substituents in Oxazolones

Gülsiye Öztürk · Hasan Karabıyık · Muhittin Aygün · Serap Alp · Serdar Özçelik

Received: 4 November 2012 / Accepted: 24 February 2013

Abstract The solvatochromic and spectral properties of oxazolone derivatives in various solvents were reported. Fluorescence spectra clearly showed positive and negative solvatochromism depending on substituents. The solvatochromic plots and quantum chemical computations at DFT-B3LYP/6-31+G(d,p) level were used to assess dipole moment changes between the ground and the first excited singlet-states. The electron accepting nitro substituent at the para-position increased the π-electron mobility, however, the 3,5-dinitro substituent decreased the π-electron mobility as a result of inverse accumulation of the electronic density as compared with that of its ground state. Experimental and computational studies proved that the photoinduced intramolecular electron transfer (PIET) is responsible for the observed solvatochromic effects. We demonstrate that PIET can be finely tailored by the position of the electron accepting and donating substituents in the phenyl ring of the oxazolone derivatives. We propose that the photoactive CPO derivatives are new molecular class of conjugated push-pull structures using azlactone moiety as the π-conjugated linker and may find applications in photovoltaic cells and light emitting diodes.

Keywords Solvatochromism · Photoinduced Intramolecular Electron Transfer (PIET) · Stokes shift · Hypsochromic shift · Bathochromic shift · Azlactone

Introduction

Solvatochromism, inherently dynamical phenomenon, is universally exploited to probe chemical and biological properties of molecules in various environments. Solvatochromic effects probed by spectroscopic techniques have been a subject of several investigations [1–15]. A change in polarity, dielectric constant or polarizability of the solvent differently causes perturbation in the ground and excited states of organic compounds. A systematic analysis of the solvent effect is, therefore, specifically informative to probe excited state behavior of the molecules. The solvatochromic effect is frequently used to determine polarity of microenvironment of peptides, proteins and lipid bilayers using an intrinsic or extrinsic fluorescence probes [16, 17]. The conjugated organic dye molecules are recognized as important materials having novel electronic and photonic properties suitable for many technological applications [6]. The spectral characteristics of an aromatic molecule are dependent on the nature as well as on the position of the substituent in the aromatic ring [1, 13]. Conjugated structures with electron donor and acceptor substituents have attracted considerable attention because of their remarkable photoinduced intramolecular electron transfer (PIET) processes and their related second-order non-linear optical (NLO) response. Promising applications of conjugated structures can be exemplified as polymer-made modulators, amplifiers, elements for optical information recording, telecommunication devices, and optical switches [18–22].

Macro-cyclic molecules have been used in a variety of chemical processes, e.g., selective complexing agents for metals, PIET, bio-mimetric studies, etc. [9]. Crown ether

Electronic supplementary material The online version of this article (doi:10.1007/s10895-013-1198-6) contains supplementary material, which is available to authorized users.

G. Öztürk · S. Alp
Department of Chemistry, Dokuz Eylül University, 35160 Izmir, Turkey

H. Karabıyık (✉) · M. Aygün
Department of Physics, Dokuz Eylül University, 35160 Izmir, Turkey
e-mail: hasan.karabiyik@deu.edu.tr

S. Özçelik
Department of Chemistry, Izmir Institute of Technology, 35430 Izmir, Turkey

derivatives are prominent among such macro cyclic molecules [23]. There is a growing interest in crown ether derivatives fused with fluorophores. These derivatives show marked changes on metal complexation and interesting properties like excimer/exciplex formation. Such modifications increase the selectivity and sensitivity of crown ethers for metal ions. Moreover, they are candidate materials as colorimetric analytical agents and indicators for metal ions.

Azlactones have wide range of applications as precursors for synthesis of some organic compounds, such as amino acids, peptides, anti microbial or antitumor compounds [24–29] and polymers [30–32]. They have also been used to prepare metal chelates with transition metal ions [33] and charge transfer complexes [34]. Another important application includes their use in non-linear optical materials [35]. The fluorescence quantum yield of the aryl derivatives of 5-oxazolones in solid-state was found to be much higher in comparison to the solutions [36]. It is suggested that very low fluorescence quantum yields of azlactones in solution are not caused by only intersystem crossing from S_1^* ($\pi\,\pi$) to T^* (n π) states, but possibly some photochemical diabetic process that acts in the excited singlet state, and is followed by a reverse reaction into the ground state, solvation and steric effects that result in non-planarity of the molecular system [37]. High fluorescence quantum yields in the solid state are attributed to the planarity of the azlactone molecule upon packing into the crystal lattice and consequent prevention of any intramolecular rotations and vibrations.

We synthesized several 5-oxazolone derivatives and characterized their sensor responses by spectroscopic techniques [36–42]. We recently synthesized 5-oxazolone derivatives which contain an *N*-phenyl-(aza-15-crown-5) moiety shown in Scheme 1 [43]: 2-phenyl-4-[4-(1,4,7,10-tetraoxa-13-azacyclopentadecyl) benzylidene]-5-oxazolone (CPO-1), 2-(3,5-dinitrophenyl)-4-[4-(1,4,7,10-tetraoxa-13-azacyclopentadecyl)benzylidene]-5-oxazolone (CPO-2), 2-(4-nitrophenyl)-4-[4-(1,4,7,10-tetraoxa-13-azacyclopentadecyl) benzylidene]-5-oxazolone (CPO-3) and 2-(4-tolyl)-4-[4-(1,4,7,10-tetraoxa-13-azacyclopentadecyl)benzylidene]-5-oxazolone (CPO-4) derivatives. We specifically concentrate to elucidate molecular mechanism of PIET depending on electron accepting and donating substituents. The present study systematically explores how electron accepting and donating substituents affect electron transfer processes in oxazolones.

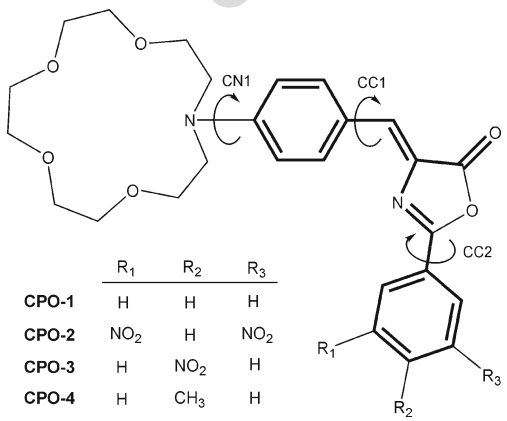

	R_1	R_2	R_3
CPO-1	H	H	H
CPO-2	NO_2	H	NO_2
CPO-3	H	NO_2	H
CPO-4	H	CH_3	H

Scheme 1 The CPO derivatives used in the present study showing allowed rotations around single bonds of π-conjugated linker. Conjugated paths on (Z)-4-benzylidene-2-phenyloxazol-5(4H)-one bridge are marked with *bold lines*

Experimental

Materials and Equipment

Absorption measurements were carried out with Varian-Cary spectrophotometer, and fluorescence measurements were made by using Varian-Cary Eclipse spectrofluorimeter. Synthesis, purification and basic characterization of the CPOs were described in our previous study [43]. All solvents used were spectroscopic grade available commercially. All experiments were carried out at the room temperature.

Photophysical Properties

Fluorescence quantum yields (Φ_F) were determined by the comparative method [44, 45]:

$$\Phi_F = \Phi_{std} \times \left(F\, A_{std}\eta^2\right)/\left(F_{std} A\, \eta_{std}{}^2\right), \quad (1)$$

where F and F_{std} are the areas under the fluorescence emission curves of the samples and the standard, respectively. A and Astd are the respective absorbances of the samples and standard at the excitation wavelength, respectively, and η and η_{std} the refractive indexes of solvents used for the samples and standard, respectively. Rhodamine 101 (in Ethanol) (Φ=1) [46, 47] was employed as the standard.

The radiative lifetime, τ_0, was estimated by the formula, [48, 49] assuming the lowest singlet state is the only fluorescent state:

$$\tau_0 = 3.5 \times 10^8 / \nu^2{}_{max}\varepsilon_{max}\Delta\nu_{1/2} \quad (2)$$

where ν_{max} is the wave number in cm^{-1}, εmax is the molar extinction coefficient at the selected absorption wavelength, and $\Delta\nu_{1/2}$ is the half width of the selected absorption in wave number units of cm−1.

The fluorescence lifetime (τ_f) is calculated by the formula given below:

$$\Phi_F = \tau_f/\tau_0 \quad (3)$$

The radiative, kr, and nonradiative, knr, rate constants were calculated from the fluorescence quantum yield and radiative lifetimes by using:

$$k_r = \Phi_F/\tau_f = 1/\tau_0 \quad (4)$$

$$k_{nr} = (1-\Phi_F)/\tau_f = 1 - k_r \quad (5)$$

Methodological Procedure

Using the well-established fluorescence solvatochromic method, dependence of Stokes shifts of the CPO derivatives considered in this study can be used to determine the magnitudes as well as directions of electric dipole moment of solute molecules in the first electronically excited state. In this regard, the measured absorption and emission spectra of the CPO derivatives within different solvents (dimethylsulfoxide-DMSO, tetrahydrofuran-THF, toluene, chloroform, dichloromethane-DCM, acetonitrile-ACN) whose permitivities range from 2.37 to 46.82 were analyzed by considering the dipole-dipole interaction of the polarized excited state within the solvents. In this study, Bakhshiev's solvathochromic theory has been used to estimate the first excited state dipole moments of the considered fluorophores [50, 51]. The variations of the Stokes shifts $\Delta\nu=(\nu_a - \nu_f)$ against the solvent polarizability function $f(\varepsilon,n)$ allow for determination of the difference between the excited state and ground state dipole moments, $\Delta\mu=(\mu_e - \mu_g)$ within a linear regime:

$$\Delta\nu = \nu_a - \nu_f = \frac{2}{hca^3}\left(\mu_e - \mu_g\right)^2 f(\varepsilon,n) + const. \quad (6)$$

where

$$f(\varepsilon,n) = \left(\frac{\varepsilon-1}{\varepsilon+2} - \frac{n^2-1}{n^2+2}\right) \times \frac{2n^2+1}{n^2+2} \quad (7)$$

in Bakhshiev's theory. Here n, ε and a stand for the refractive index, permitivity of the solvents and the radius of spherical Onsager cavity surrounding the dipole moment of fluorophore molecule, respectively. The slope (s) of such plots provides a direct access to the excited state dipole moment according to the following equation

$$\left(\mu_e - \mu_g\right)^2 = \frac{hcsa^3}{2}. \quad (8)$$

Thus, one can easily calculate the difference between the excited state and the ground state dipole moments as follows;

$$\mu_e - \mu_g = 0.01\sqrt{sa^3}, \quad (9)$$

where a, s and dipole moments are expressed in Å, cm^{-1} and debye, respectively.

Changes in dipole moments obtained from such plots depend strongly on the ground state dipole moments (μ_g) besides Onsager radius a. Onsager radii are roughly equated to the molecular van der Waals radius or calculated by Suppan equation [52] within a macroscopic framework. This approximation to determine Onsager radius cannot be acceptable for the ellipsoidal (or elongated) fluorophores [53]. It is obvious that the uncertainty in the estimation of a results in questionable accuracy [54]. Therefore, to properly determine solute molecules' dipole moment cavity radii a and the ground state dipole moments, volume and dipole moment calculations on the optimized geometries of the fluorophores in different solvents were performed by means of self-consistent-reaction-field (SCRF) calculations [55–58] including the solvent stabilization energies into the Hamiltonian of the systems according to Polarizable Continuum Model (PCM) [59, 60]. While choosing the solvents to be included in the calculations, their polarizability functions (f) are considered. Six solvents whose polarizabilities vary in a wide range (0.028 for toluene, 0.363 for chloroform, 0.543 for THF, 0.590 for CH_2Cl_2, 0.841 for DMSO and 0.859 for acetonitrile) are used in the calculations. The remaining three solvents, xylene (f=0.031), ethylacetate (f=0.489) and DMF (f=0.837) are excluded, since their polarizabilities are close to that of toluene, THF and DMSO, respectively. The volume calculations within the considered solvents and geometry optimizations of the dyes were performed by Density Functional Theory with the use of Becke's three-parameters hybrid exchange-correlation functional (B3LYP) [61] incorporating B88 gradient-corrected exchange [62] and Lee–Yang–Parr non-local correlation functional [63] by means of 6-31+G(d,p) basis set implemented in Gaussian 03 W program package [64]. In addition, solvation free energies of the solutes in the considered solvents are computed as the sum of several components such as electronic, dispersion, repulsion, polarized solute-solvent, cavitation and non-electrostatic energy terms [65].

In order to quantitatively express π-electron mobility of 4-benzylideneoxazol-5-one acted as bridge linking donor fragment (crown ether) with acceptor fragment (substituted phenyl), topological analyses on the electron density distribution $\rho(\mathbf{r})$ for each of the considered fluorophores were performed. For this purposes, wavefunction sets corresponding to CPOs are obtained by Kohn-Sham molecular orbitals. Then, they are used as input data to AIM2000 software [66] to calculate the delocalization indices (DIs) in the framework of the Quantum Theory of Atoms in Molecules (QTAIM) [67–69]. DI between atoms A and B, δ(A,B), is obtained by double integration of exchange or Fermi correlation between electrons, $\Gamma_{xc}(\mathbf{r}_1,\mathbf{r}_2)$, over the atomic basins Ω_i and Ω_j:

$$\delta(i,j) = -2\int_{\Omega_i}\int_{\Omega_j} \Gamma_{xc}(\mathbf{r}_1,\mathbf{r}_2)d\mathbf{r}_1 d\mathbf{r}_2 \quad (10)$$

and can be seen as a quantitative measure of electron pair sharing between atomic basins Ωi and Ωj [70]. Orders of the bonds allowing rotation depending on excitation, which are linked crown ether nitrogen to phenyl of4-benzylideneoxazol-5-one, phenyl to oxazol and oxazol to the substituted phenyl ring, were carried out using topological parameters such as DIs of these formally single bonds according to procedure in [71].

Results and Discussion

Spectral Properties and Solvatochromism

Absorption and fluorescence spectra of the CPO derivatives in xylene are shown in Fig. 1. The photophysical properties of the derivatives in different solvents are tabulated in Table 1. The extinction coefficients of the derivatives are very high, indicating an extensive conjugation of π-electrons on the planar structure of the chromophore fragment. We confirmed the existence of planar structure of azlactone fragments by the geometry optimizations of the CPO derivatives at DFT-B3LYP/6-31+G(d,p) level. The absorption and fluorescence spectra of the CPO-2 and CPO-3 were substantially shifted to higher wavelengths. But the spectra of the CPO-4 exhibited a slight blue-shift when the spectral position of the CPO-1 was taken as reference. The spectra were bathochromically shifted when the electron accepting nitro groups was inserted in the para- and meta- positions of the phenyl ring. On the other hand, the addition of the electron donating methyl group in the para- position of the phenyl ring caused a slight hypsochromic shift in the absorption and emission maxima of the CPO-4 derivative. These findings indicated that the nature and specifically the positions of the nitro and methyl groups strongly modulated the spectral properties of the CPO derivatives. We propose that the position of the electron accepting or donating groups attached to chromophore of the oxazolones tunes the electronic energy levels of the CPO derivatives.

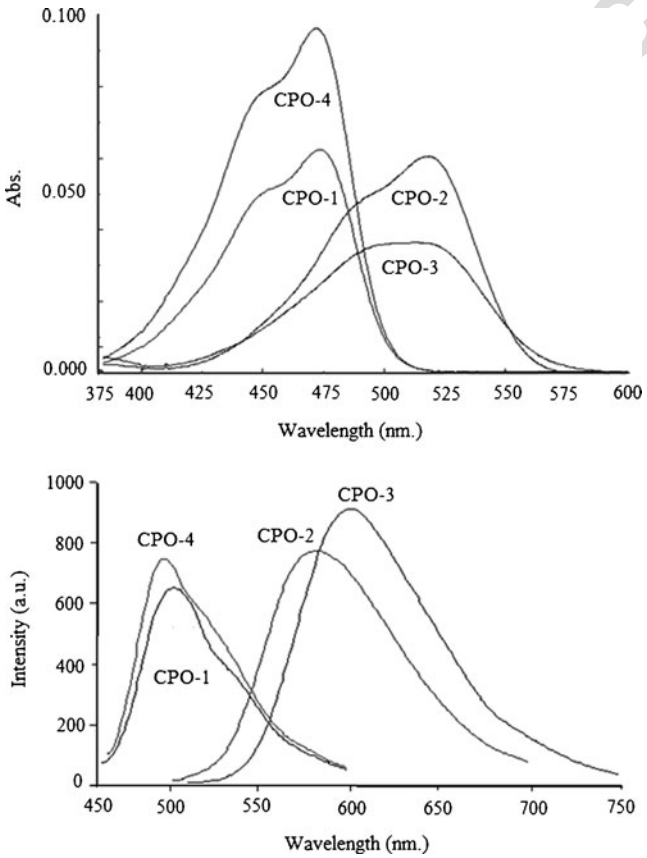

Fig. 1 Absorption and fluorescence spectra of the CPO derivatives in xylene. Spectra indicate strong influence of the substituents

Excited state properties can be evaluated by measuring fluorescence quantum yields of the CPO derivatives in various solvents. Fluorescence quantum yields (QYs) of the derivatives are quite low ($\phi_F << 1.0$ %) in most of the solvents used in this study (Table 1). The only exception is that the QY of the CPO-3 in toluene is moderate (> 10 %). The fluorescence QYs of the CPO-2 and CPO-3 derivatives in some solvents were below the detection limit of the instrument used in this study. The rank for the QYs in the same solvent is as CPO-3>CPO-1~CPO-4>CPO-2. However, there is no clear trend observed for the QYs with the solvent polarizability. The effects arising from rotational and vibrational degrees of freedom for the derivatives are predominant in polar solvents, leading to non-radiative transitions, which are extremely fast causing vanished quantum yields. The bond orders may be related to rotations of formally single bonds shown in Scheme 1. The calculated bond orders have been given in Table 2. As the bond order increases the rotations around that bond are hindered. Consequently, the relationship among the orders of CN1 and CC1 shown in Scheme 1 comply with the QYs of CPO derivatives. Furthermore, the bond orders indicate that the rotations around CC2 bond have limited effect on the excited state geometries of the CPOs. Since the QY is very weak in solvent the charge transfer should be highly effective by reducing the rate of radiative transitions. The radiative lifetimes and the rate constants of the CPO derivatives were estimated by using Eqs. 2–5 because the quantum yields are very low making lifetime measurements very difficult and unreliable. The rank of the radiative lifetime, CPO-3>CPO-1~CPO-4>CPO-2, correlates with the rank of quantum yield, verifying low radiative rate constants (Table 1).

The ground and excited states as well as the transition dipole moments of the derivatives in various solvents were calculated as listed in Table 3. The ground state dipole moments of the derivatives were increased in polar solvents. Moreover, the ground state dipole moments for the nitro substituted derivatives were amplified (more than 50 % in magnitude), but decreased for the CPO-4 derivative having the methyl group. The excited-state dipole moments of the

Q1/Q4

Table 1 Photophysical parameters of the CPO derivatives in different solvents: λ (nm); ε (10^4 $lmol^{-1}cm^{-1}$); Stokes shifts (Δν, cm^{-1}); fluorescence quantum yield (ϕ_F); radiative lifetime, τ_0 (ns); fluorescence rate constants k_r ($10^9 s^{-1}$); k_{nr} ($10^9 s^{-1}$). Solvents are listed in their order of polarizability

Solvent	$\lambda^{abs}{}_{max}$	ε_{max}	$\lambda^{emis}{}_{max}$	ϕ_F	Δν	τ_0	k_r	k_{nr}
CPO-1								
TOL	473	6.0	507	0.0037	1418	0.078	12.80	3447.4
XYL	473	6.3	502	-	1221	0.071	-	-
CHLF	475	6.0	517	0.0028	1710	0.082	12.23	3335.1
ETAC	469	5.8	517	0.0043	1980	0.083	12.05	2789.1
THF	472	12.7	516	0.0048	1807	0.060	16.67	3455.6
DCM	472	7.6	524	0.0011	2102	0.037	26.82	24363
ACN	469	8.8	536	0.0039	2665	0.031	32.23	8232.2
DMF	478	5.6	541	0.0056	2436	0.098	10.20	1811.3
DMSO	483	12.2	548	0.0064	2456	0.037	27.00	4192.4
CPO-2								
TOL	518	6.4	584	0.0129	2182	0.106	9.44	722.1
XYL	517	6.0	580	-	2101	0.109	-	-
CHLF	524	7.0	580	-	1843	0.106	-	-
ETAC	506	6.3	653	0.0006	4449	0.426	2.34	3903.9
THF	509	57.1	558	0.0002	1725	0.012	100	499900
DCM	517	52.0	570	-	1799	0.016	-	-
ACN	504	55.7	554	-	1791	0.012	-	-
DMF	512	5.2	560	-	1674	0.146	-	-
DMSO	516	16.2	615	-	3120	0.035	-	-
CPO-3								
TOL	508	5.6	603	0.1155	3101	0.133	7.54	57.6
XYL	508	9.6	600	-	3018	0.076	-	-
CHLF	516	4.9	654	-	4089	0.171	-	-
ETAC	505	5.2	689	0.0207	5288	0.137	7.30	345.3
THF	510	40.3	663	0.0064	4525	0.021	47.76	7414.9
DCM	515	46.3	669	-	4470	0.018	-	-
ACN	505	47.8	675	-	4987	0.017	-	-
DMF	515	4.4	572	-	1935	0.199	-	-
DMSO	522	12.6	728	-	5421	0.055	-	-
CPO-4								
TOL	471	6.6	498	0.0037	1151	0.071	14.07	3788.2
XYL	472	9.6	496	-	1025	0.046	-	-
CHLF	473	9.1	513	0.0028	1648	0.059	46.97	6043.6
ETAC	467	9.4	515	0.0036	1996	0.051	19.56	5415.2
THF	472	72.4	520	0.0044	1956	0.007	141.9	32116
DCM	474	75.4	523	0.0011	1977	0.007	137.5	124862
ACN	468	68.7	533	0.0035	2606	0.007	140	39860
DMF	476	8.9	537	0.0056	2386	0.059	16.97	3013.3
DMSO	482	13.9	544	0.0065	2365	0.032	31.25	4776.4

TOL Toluene, *XYL* Xylene, *CHLF* Chloroform, *ETAC* Ethyl acetate, *THF* Tetrahydrofuran, *DCM* Dichloromethane, *ACN* Acetonitrile, *DMF* Dimethylformamide, *DMSO* Dimethylsulfoxide

CPO-3 derivative were significantly increased by the presence of the nitro groups. Nevertheless, the excited states dipole moments of the CPO-2 were drastically lowered about 9D compared to the CPO-3. The transition dipole moments were found to large and positive for the derivatives of CPO-1, CPO-3 and CPO-4. But, the sign of the transition dipole moment for the CPO-2 is negative and its absolute value was dropped off with the increasing polarizability of solvent. This remarking difference is therefore attributed to the electron accepting

Table 2 The orders of formally single bonds allowing rotations around themselves shown in Scheme 1

	CN1	CC1	CC2
CPO-1	1.061	1.200	1.041
CPO-2	1.080	1.223	1.023
CPO-3	1.074	1.216	1.034
CPO-4	1.069	1.204	1.038

Table 3 Calculated Onsager radii (in Å), ground and excited state dipole moments (in debye) of the considered CPO derivatives within different solvents. Solvents are listed in their order of polarizability according to Bakhshiev's theory (f')

Solvent	Onsager Radii (a)				Ground State Dipole Moments (μ_g)				$\Delta\mu_{ge}=\mu_e-\mu_g$				Excited State Dipole Moments (μ_e)			
	CPO-1	CPO-2	CPO-3	CPO-4	CPO-1	CPO-2	CPO-3	CPO-4	CPO-1	CPO-2	CPO-3	CPO-4	CPO-1	CPO-2	CPO-3	CPO-4
TOL	6.17	5.85	5.80	5.90	4.864	7.799	7.257	4.694	5.819	−4.010	6.972	5.794	10.683	3.789	14.235	10.488
CHLF	5.86	5.90	6.10	5.92	5.165	8.065	7.574	4.981	5.386	−3.897	7.527	5.824	10.551	4.168	15.101	10.805
THF	6.12	5.90	6.16	6.01	5.277	8.156	7.714	5.089	5.748	−3.814	7.638	5.957	11.025	4.342	15.353	11.046
DCM	5.98	5.67	5.80	5.79	5.319	8.176	7.760	5.132	5.552	−3.223	6.978	5.633	10.871	4.953	14.738	10.765
DMSO	5.71	6.12	6.18	6.13	5.485	8.319	7.924	5.286	5.180	–	7.676	6.136	10.665	–	15.599	11.423
ACN	6.03	6.02	5.67	6.20	5.486	8.308	7.934	5.289	5.622	−4.020	6.745	6.242	11.108	4.288	14.679	11.531

nature and the position of nitro groups. The electron-accepting nitro groups at the para and meta positions strongly modulate the sign and the magnitude of the transition dipole moments, by causing reversal in the direction of dipole moment vector. These computational findings confirm that the charge redistribution upon photo-excitations can be tuned by nature and position of the substituents.

The internal rearrangement of electrons (charge redistribution) upon optical excitation can be clearly verified by the solvent effects. The solvatochromic plot by depicting the amount of change in Stokes shifts against Bakhshiev's orientational polarizability of solvents was shown in Fig. 2a. By

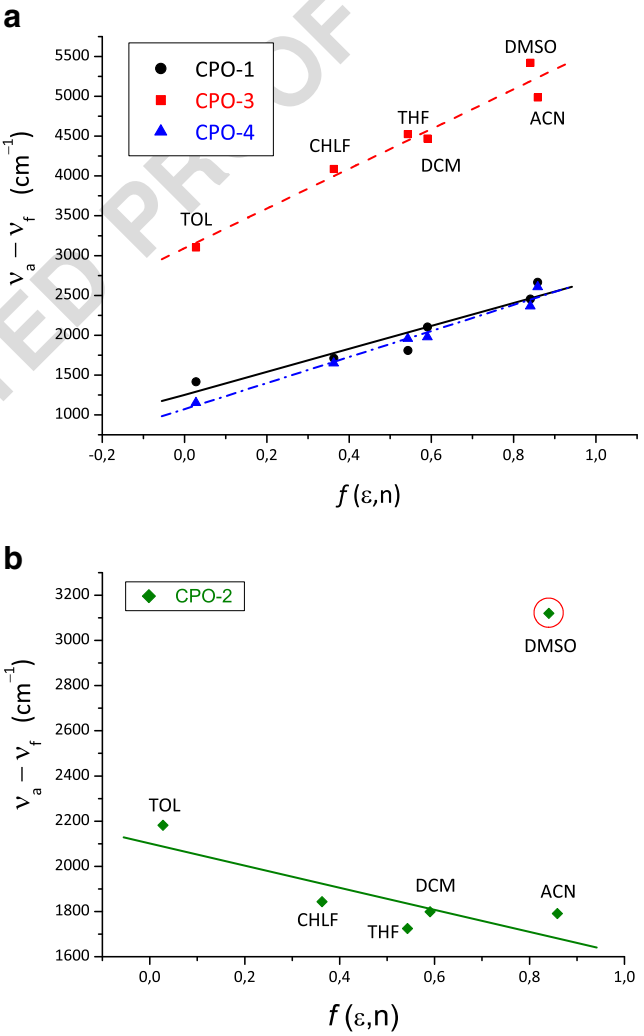

Fig. 2 **a** Plots of the Stokes shifts against solvent polarizability function f (ε,n) for CPO-1 (*filled circles*), CPO-3 (*filled squares*) and CPO-4 (*filled triangles*). Linear correlations between the Stokes shifts ($\nu_a - \nu_f$) and solvent polarizability functions (f) are expressed as ($\nu_a - \nu_f$)= 1441.49 f+1252.19 (R=0.953) for CPO-1 (*solid line*); ($\nu_a - \nu_f$)= 2496.06 f+3091.55 (R=0.977) for CPO-3 (*dashed line*); ($\nu_a - \nu_f$)= 1634.77 f+1072.37 (R=0.989) for CPO-4 (*dash-dotted line*). **b** Plots of ($\nu_a - \nu_f$) against f (ε,n) showed by filled diamonds of CPO-2. Linear correlation by eliminating the DMSO data which shows much deviation is expressed as ($\nu_a - \nu_f$)=−489.38 f+2101.17 (R=− 0.832)

changing solvent from a low polar toluene to a high polar acetonitrile, the Stokes shifts was increased with the associated slopes of 1,441, 2,496 and 1,634 cm^{-1} for the CPO-1, CPO-3 and CPO-4 derivatives, respectively. The results point that the general solvent effects are operative for these derivatives. However, the CPO-2 derivative displayed a noteworthy exception as shown in Fig. 2b. Even though the CPO-2 is the most polar derivative in the ground state according to the dipole moment values given in Table 2, the solvatochromic plot for the CPO-2 derivative illustrates a plot with a diminutive slope with increasing solvent polarizability. As a result of that the fluorescence spectra of the CPO-2 derivative shifted to lower wavelengths with increasing solvent polarizability (Table 2 and the supporting information). This is known as negative solvatochromism [72–74]. The attachment of electron-accepting nitro groups at the meta positions of the phenyl ring caused decreasing Stokes shift with increasing polarizability. But, when the electron accepting nitro group introduced at the para position, very large and positive Stokes shift with increasing polarizability was observed. The presence of electron donating methyl group was not induced strong solvatochromic behavior compared to the CPO-1. In addition, it has been illustrated that the solvent DMSO interacted with the CPO-2 molecules, generating a deviation from the linearity of the plot. This deviation is attributed to the specific solvent effect [75, 76]. However, acetonitrile almost having the same orientational polarizability as DMSO does not facilitate the specific solvent effect. Even it is elusive, this might be explained by H-bonding between methyl groups in DMSO with the nitro groups in the CPO-2 derivative. The observed solvatochromism strongly associates with the position and the nature of electron accepting/donating groups in the phenyl ring; and verify that the photoinduced intramolecular electron transfer takes place and the transfer can be tuned by the position and the nature of the substituent.

Photo-Induced Intramolecular Electron Transfer (PIET)

PIET, a phenomenon, is observed when there is a substantial change in intramolecular charge distribution, evidenced by solvent effects [77] or dipole moment measurements/calculations [78]. It is well known that very large Stokes shifts originate from charge transfer between donor and acceptor parts of a molecule connected through conjugated π-bonds. In our case, the 4-benzylideneoxazol-5-one acts as electron transmitter in the PIET process between the donor crown ether and the acceptor substituted phenyl groups (Scheme 1). The presence of electron accepting nitro groups causing red-shift in the absorption and emission spectra initiated strong intramolecular electron transfer. In this section, we aim to elaborate the relations among energy level, molecular structure and PIET. Figure 3 illustrated the

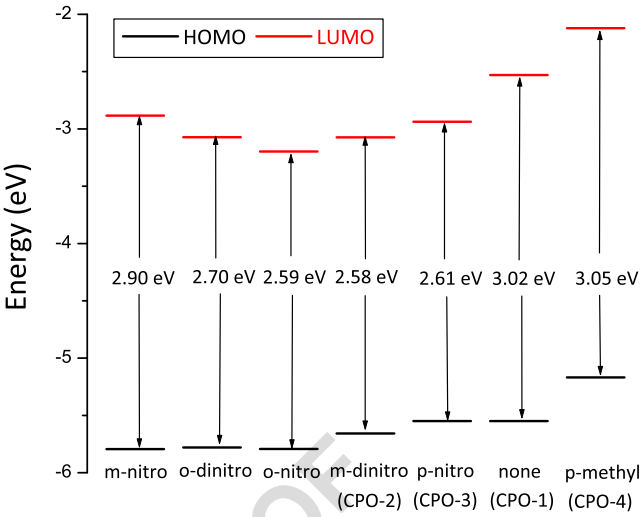

Fig. 3 Frontier molecular orbital energy levels of the CPO derivatives and three hypothetical variants, *m*-nitro, *o*-nitro and *o*-dinitro. The nature and the positions of the substituents modulate the energy levels

calculated HOMO and LUMO energy levels, and the band-gap of the derivatives including three hypothetical variants m-nitro, o-nitro and o-dinitro. The unsubstituted derivative, the CPO-1 has the band gap energy of 3.02 eV. Both the HOMO and LUMO levels of the p-methyl substituted CPO-4 derivative were strongly shifted to higher energy levels due to the electron donating ability of the methyl to the chromophore. The resulting band gap energy was also slightly increased, about 0.03 eV, generating very slight blue shift in the optical spectra. The HOMO levels for the derivatives carrying the nitro groups were weakly affected by the position of the electron accepting nitro groups but the LUMO levels were strongly modulated. The calculated HOMO-LUMO energy band gaps for the nitro substituted derivatives were found to be up to - 0.44 eV. This very large reduction in the band gap energy due to presence of the electron accepting nitro groups were yielded strong red-shifts observed in the spectra, confirming the experimental assignments. The calculations indicate that the presence of electron donating methyl substituent slightly influence the PIET because the band gap energy was barely increased. The presence of electron accepting nitro derivatives should facilitate PIET due to reduced HOMO-LUMO band gap energy. Therefore, we propose that PIET can be tuned by the position and the nature of substituent groups, i.e. electron accepting or donating.

It is imperative to demonstrate that the electron delocalization and the partial charges on the substituted phenyl moiety maybe able to control the energy levels and PIET. The frontier molecular orbitals (FMO) of the CPO derivatives were depicted in Fig. 4. The HOMO levels of the FMO

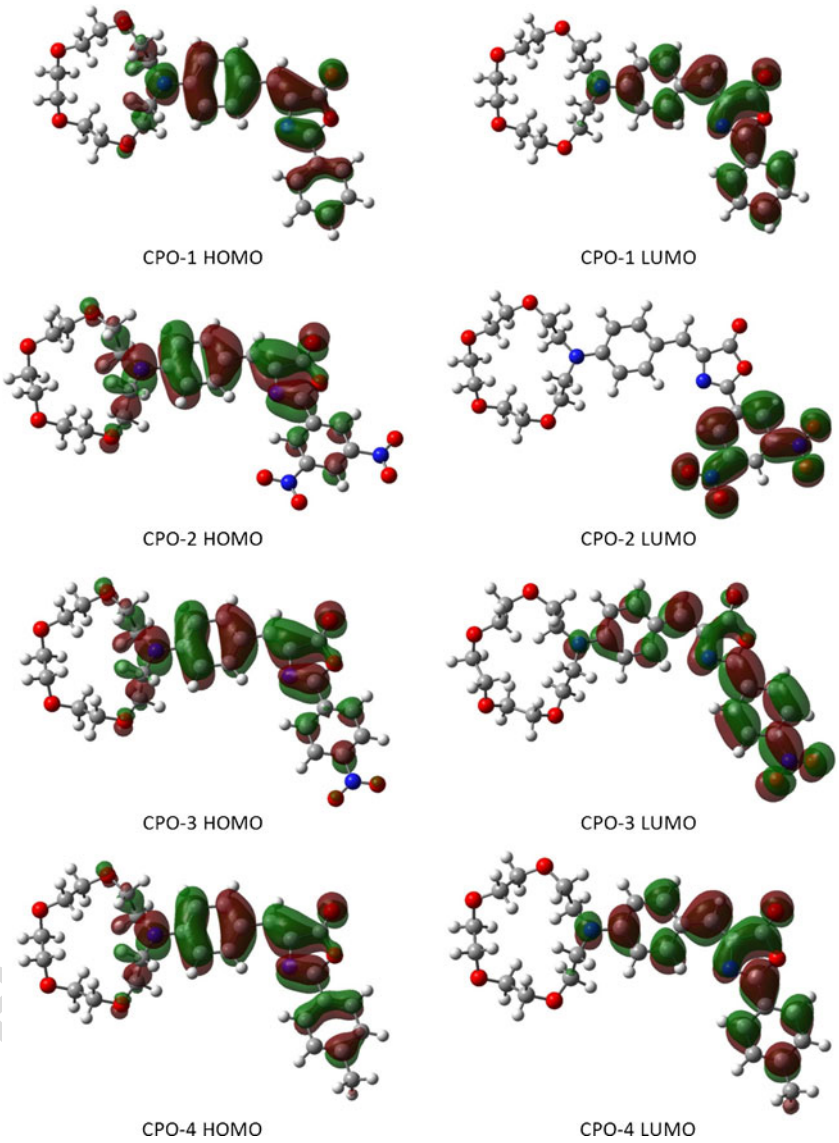

Fig. 4 Isodensity surfaces of the frontier molecular orbitals of the CPOs at the isovalue of 2×10^{-2} in a reference medium (vacuum)

clearly present that the π-electrons were mostly delocalized over the conjugation bridge and on the nitrogen atom of the crown ether ring. The nitro substituent were changed the extent of the delocalized orbitals but the methyl group did not make any impact on the orbitals. The similarity of the FMO of the CPO-1 and CPO-4 is evident, indicating that the same type of transition between the HOMO and LUMO energy levels should occur. The spectral resemblance of the derivatives (Fig. 1) is clearly seen. But, the FMO of the CPO-2 derivative at the LUMO level is quite different. The excited electrons were totally localized on the nitro substituted phenyl ring. This unusual behavior in the CPO-2 derivative arises from the localization of the electrons at the meta positions because of the presence of two electron-accepting nitro groups. Electrons in the LUMO level flows in opposite directions due to the strong electron accepting nitro groups at the 3, 5 positions of the phenyl ring, causing localized partial charges on the phenyl ring (Scheme 2). Because of this localized partial charges the direction of the dipole moment in the excited state is reversed and the sign of the transition dipole moment becomes negative. This reversal is the origin of the negative solvatochromism observed for the CPO-2 derivative. On the other hand, the CPO-3 derivative possesses larger dipole moments due to more polarized π-electrons in the excited-state, yielding the positive solvatochromism.

The partial charges on the substituted phenyl ring shed more lights on the origin of the localized electrons for the CPO-2 derivative. The Scheme 2 shows the partial charges on the ring atoms due to the resonance structures. The effect of electron accepting nitro substituents is only present on the phenyl ring because none of the resonance structures generates a partial positive charge which can be stabilized by the electron donating group (represented by R in the Scheme 2,

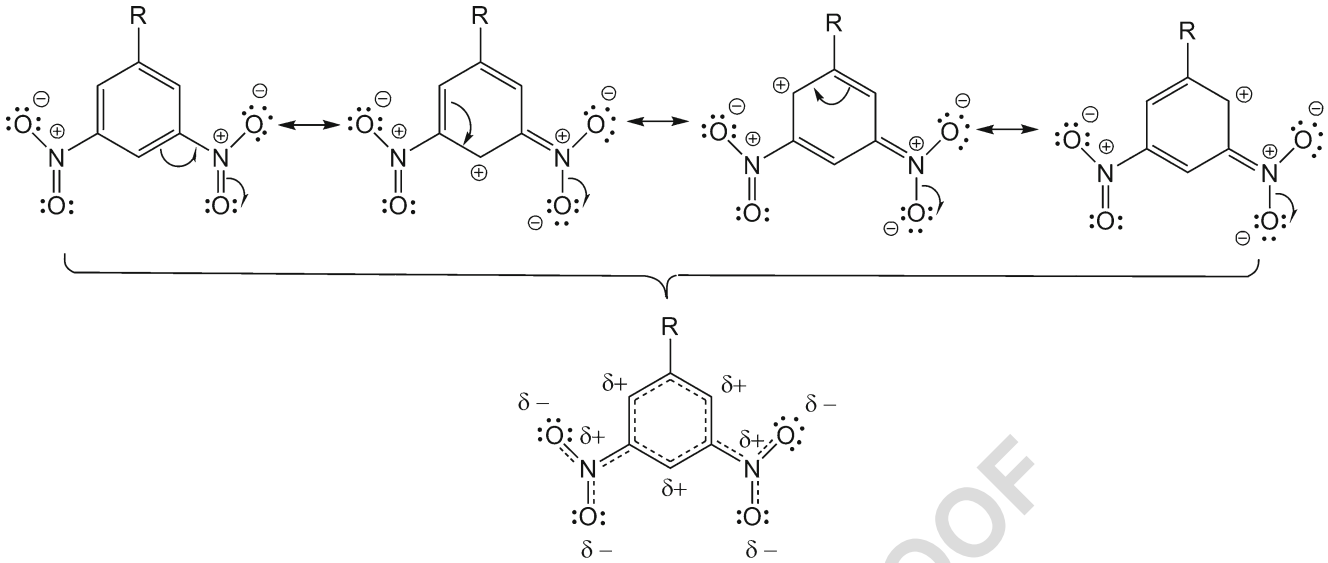

Scheme 2 The resonance structures of the CPO-2 derivative. Electron-accepting nitro gruops on the meta positions of the phenyl ring and their equivalent resonance hybrid structure. Group R includes azlactone and crown ether moiety

the crown ether and the conjugated bridge). Hence the nitro substituents not just hold the electrons on the FMO but also lower the LUMO energy levels of π-orbitals present on the phenyl ring. This unusual behavior in the CPO-2 derivative should reduce the electron mobility in the conjugated bridge, explaining the negative solvatochromism.

Electron mobility occurred in the excited states of the CPOs can be inferred from the frontier molecular orbitals as depicted in Fig. 4. The non-bonding electrons on the nitrogen of crown ether moiety contribute towards the mobility of the π-electrons on the phenyl ring. While the p-methyl substituent in the CPO-4 does not initiate a considerable change in the π-electron mobility, the nitro substituent in the CPO-2 and CPO-3 derivatives strongly affect the flow of the π-electron density. It is worth noting that there is a deficiency in π-electron mobility of the CPO-2 (Fig. 4) as compared to the other CPOs due to the lack of linkage between FMOs, localized on the nitro groups, forming strong electrophilic regions. As a result, the charge separation capability of the CPO-2 is considerably decreased relative to the other CPOs. It is therefore reasonable that the excited state dipole moments of the CPO-2 are lower than those of the ground states of the CPO-2 because of electronic charge depletion in the associated LUMO level since the dipole moment of a molecule depends on its electron density. The FMOs of the CPO-2 scarcely overlap as shown in Fig. 4 and consequently the dipole moment vector in the excited state of CPO-2 is reversed depending on PIET. This fact explains the lower dipole moment values in the excited states of the CPO-2 having the nitro groups at the 3, 5 positions. The crown ether moiety behaves as π-donor (D) and the substituted phenyl moiety acts as π-acceptor (A) in the CPO derivatives. Since the CPO derivatives show evidence of substitution-induced photophysical properties and PIET, we propose that the photoactive CPO skeleton is a new molecular class of conjugated push-pull structures (D-π-A) using 4-benzylideneoxazol-5-one as π-conjugated linker.

The π-electron mobility of the derivatives can be also inferred from the slopes of the solvatochromic plots (Fig. 2). Considering the CPO-1 as a reference compound, the π-electron mobility of the CPO-3 and CPO-4 derivatives is increased by the presence of electron accepting/donating groups at the 4-position (the para-position) of the phenyl ring, whereas the 3,5-dinitro substituent decreases the π-electron mobility. Moreover, the electron accepting nitro substituent at the 4-position increases π-electron mobility much more than the electron donating methyl substituent at the same position. These inferences are further verified by the results from average delocalization index (DI) calculated on the conjugated paths shown in Scheme 1. Average DIs for the CPO-1, CPO-2, CPO-3 and CPO-4 were calculated as 1.274, 1.268, 1.280 and 1.278, respectively. Average DI can be taken as an acceptable measure for the π-electron mobility on the π-conjugated linker, 4-benzylideneoxazol-5-one, between the donor and acceptor fragments since the rank of average DI is the same as the rank of the slopes in the solvatochromic plots. The very large Stokes shifts of the CPO-3 indicate that the PIET is the highest among the CPOs.

Conclusions

We examined the molecular mechanism of the PIET in four oxazolone derivatives in various solvents. Highly strong

spectral red shifts for the CPO-2 and CPO-3 derivatives and a slight blue-shift for the CPO-4 derivatives were observed depending on the position and the nature of the substituents. The spectral shifts were assigned to the transitions upon photo-induced electron transfers from the nitrogen of the crown ether moiety (electron donating group) to the phenyl group (electron accepting group) of the oxazol-5-one moiety. The CPO-3 and CPO-4 showed positive solvatochromism, nonetheless, the CPO-2 having *meta*-dinitro substituent has displayed a negative solvatochromic behavior. As a results of the substituent position both the ground and excited state dipole moments are regulated. The presence of electron accepting or donating groups at *para*-position of the phenyl ring increased π-electron mobility in the CPO derivatives, whereas *meta*-dinitro substituent decreased π-electron mobility due to inverse accumulation of the electronic density. The electron distribution in the frontier orbitals and the mobility of electrons are precisely controlled by the position of the electron accepting nitro groups in the derivatives. We conclude that the nature (electron acceptor or donor) and the position of the substituents on the phenyl moiety strongly modulate the energy levels, the HOMO-LUMO band gap, solvatochromic properties. We demonstrate that molecular design by the electron accepting substituent finely tunes the photo-induced intra-molecular electron transfer. Furthermore, we propose that the photoactive CPO derivatives are new molecular class of conjugated push-pull structures with 4-benzylideneoxazol-5-one moiety as π-conjugated linker. These new push-pull structures may find applications in photovoltaic devices and light emitting diodes as a molecular material regulating charge transfer [79, 80].

Acknowledgments One of the authors HK is thankful to The Scientific and Technological Research Council of Turkey (TÜBİTAK) for financial support. The work is supported by TÜBİTAK, grant (No. 112T636).

References

1. Stalin T, Sivakumur G, Shanthi B, Sekar A, Rajendrian N (2006) J Photochem Photobiol A 177:144
2. Durmus M, Ahsen V, Nyokong N (2007) J Photochem Photobiol A 186:323
3. Queiroz M-JRP, Castanheira EMS, Pinto AMR, Ferreira ICFR, Begouin A, Kirsch G (2006) J Photochem Photobiol A 181:290
4. El-Sayed M, Blaudeck T, Cichos F, Spange S (2007) J Photochem Photobiol A 185:44
5. Guzow K, Szabelski M, Karolczak J, Wiczk W (2005) J Photochem Photobiol A 170:215
6. Raikar US, Renuka CG, Nadaf YF, Mulimani BG, Karguppikar AM, Soudagar MK (2006) Spectrochim Acta A 65:673
7. Bondarev SSL, Tikhomirov SA, Knyukshto VN, Turban AA, Ischenko A, Kulinich AV, Ledoux I (2007) J Lumin 124:178
8. Benali B, Lazar Z, Elblidi K, Lakhrissi B, Massouri M, Elassyry A, Cazeau-Dubroca C (2006) J Mol Lipids 128:42
9. Kapoor S, Sapre AV, Kumar S, Mashraqui SH, Mukherjee T (2005) Chem Phys Lett 408:290
10. Chauke V, Ogunsipe A, Durmuş M, Nyokong T (2007) Polyhedron 26:2663
11. Singh RB, Mahanta S, Guchhait N (2007) Chem Phys 331:189
12. Prieto JB, Arbeloa FL, Martinez VM, Lopez TA, Amat-Guerri F, Liras M, Arbeloa IL (2004) Chem Phys Lett 385:29
13. Sharma N, Jain SK, Rastogi RC (2007) Spectrohim Acta A 66:171
14. Guzow K, Milewska M, Wiczk W (2005) Spectrochim Acta A 61:1133
15. Ozcelik S (2002) J Lumin 96:141
16. Lakowicz JR (1999) Principles of fluorescence spectroscopy. Kluwer Academic/Plenum Publishers, New York
17. Eftink MR, Ghiron CA (1976) Biochemistry 15:672
18. Prasad PN, Williams DJ (1991) Introduction to nonlinear optical effects in molecules and polymers. Wiley, Chichester
19. Chemla DS, Zyss J (1987) Nonlinear optical properties of organic molecules and crystals. Academic, Orlando
20. Mishra A, Behera RK, Behera PK, Mishra BK, Behera GB (2000) Chem Rev 100:1973
21. Spitler MT, Ehret A, Kietzmann R, Willig F (1997) J Phys Chem 101:2552
22. Ganeev RA, Tugushev RI, Ischenko AA, Derevyanko NA, Ryasnyansky AI, Usmanov T (2003) Appl Phys B 76:683
23. Gokel GW, Leevy WM, Weber ME (2004) Chem Rev 104:2723
24. Mesaik MA, Rahat S, Khan KM, Zia-Ullah, Choudhary MI, Murad S, Ismail Z, Att-ur-Rahman, Ahmad A (2004) Bioorg Med Chem 12:2049
25. Tandon M, Coffen DL, Gallant P, Keith D, Ashwell MA (2004) Bioorg Med Chem Lett 14:1909
26. Aly AA (2003) Tetrahedron 59:6067
27. Koczan G, Csik G, Csampai A, Balog E, Bosze S, Sohar P, Hudecz F (2001) Tetrahedron 57:4589
28. Bunuel E, Gil AM, Diaz-de-Villegas MD, Cativiela C (2001) Tetrahedron 57:6417
29. Grassi G, Foti F, Risitano F, Cordaro M, Nicolo F, Bruno G (2004) J Mol Struct 698:81
30. Yamashita M, Lee S-H, Koch G, Zimmermann J, Clapham B, Janda KD (2005) Tetrahedron Lett 46:5495
31. Dritina GJ, Haddad LC, Rasmussen JK, Gaddam BN, Williams MG, Moeller SJ, Fitzsimons RT, Fansler DD, Buhl TL, Yang YN, Weller VA, Lee JM, Beauchamp TJ, Heilmann SM (2005) React Funct Polym 64:13
32. Guyomard A, Fournier D, Pascual S, Fontaine L, Bardeau J-F (2004) Eur Polym J 40:2343
33. Ahmed IS, El-Mossalamy EH (2003) J Anal Appl Pyrol 70:679
34. El-Mossalamy EH, Amin AS, Khalil AA (2002) Spectrochim Acta A 58:67
35. Diaz JL, Villacampa B, Lopez-Calahorra F, Velasco D (2002) Tetrahedron Lett 43:4333
36. Ertekin K, Alp S, Karapire C, Yenigül B, Henden E, Icli S (2000) J Photochem Photobiol A 137:155
37. Icli S, Doroshenko AO, Alp S, Abmanova NA, Egorova SI, Astley ST (1999) Spectrosc Lett 32:553
38. Ozturk G, Alp S, Ertekin K (2007) Dyes Pigments 72:150
39. Icli S, Icil H, Alp S, Koc H, McKillop A (1994) Spectrosc Lett 27:1115
40. Ertekin K, Karapire C, Alp S, Yenigul B, Icli S (2003) Dyes Pigments 56:125
41. Ertekin K, Cinar S, Aydemir T, Alp S (2005) Dyes Pigments 67:133
42. Ertekin K, Alp S, Yalcin I (2005) Dyes Pigments 65:33
43. Ozturk G, Alp S, Ergun Y (2007) Tetrahedron Lett 48:7347
44. Fery-Forgues S, Lavabre D (1999) J Chem Educ 76:1260
45. Maree D, Nyokong T, Suhling K, Phillips D (2002) J Porphyrins Phthalocyanines 6:373
46. Magde D, Rojas GE, Seybold P (1999) J Photochem Photobiol 70:737

47. Broyer M, Chevaleyre J, Delacretaz G, Woste L (1984) Appl Phys B 35:31
Q3 48. Suppan P (1994) Chemistry and Light. The Royal Society of Chemistry. 70
49. Turro NJ (1965) Molecular Photochemistry, London
50. Bakhshiev NG (1964) Opt Spectrosk 16:821
51. Bakhshiev NG, Knyazhanskii MI, Minkin VI, Osipov OA, Saidov GV (1969) Russ Chem Rev 38:740
52. Suppan P (1983) Chem Phys Lett 94:272
53. Mannekutla JR, Mulimani BG, Inamdar SR (2008) Spectrochim Acta A 69:419
54. Messier J, Kajzar F, Prasad PN (1989) In: Ulrich DR (ed) Nonlinear optical effects in organic polymers. Kluwer Academic Publishers, Dordrecht
55. Wong MW, Frisch MJ, Wiberg KB (1991) J Am Chem Soc 113:4776
56. Wong MW, Wiberg KB, Frisch MJ (1992) J Am Chem Soc 114:523
57. Wong MW, Wiberg KB, Frisch MJ (1991) J Chem Phys 95:8991
58. Wong MW, Wiberg KB, Frisch MJ (1992) J Am Chem Soc 114:1645
59. Tomasi V, Cammi R, Mennucci B, Cappellia C, Corni S (2002) Phys Chem Chem Phys 4:5697
60. Tomasi J, Mennucci B, Cammi R (2005) Chem Rev 105:2999
61. Hertwig RH, Koch W (1997) Chem Phys Lett 268:345
62. Becke AD (1988) Phys Rev A 38:3098
63. Lee C, Yang W, Parr RG (1988) Phys Rev B37:785
64. Frisch MJ, Trucks GW, Schlegel HB, Scuseria GE, Robb MA, Cheeseman JR, Montgomery JA, Vreven T Jr, Kudin KN, Burant JC, Millam JM, Iyengar SS, Tomasi J, Barone V, Mennucci B, Cossi M, Scalmani G, Rega N, Petersson GA, Nakatsuji H, Hada M, Ehara M, Toyota K, Fukuda R, Hasegawa J, Ishida M, Nakajima T, Honda Y, Kitao O, Nakai H, Klene M, Li X, Knox JE, Hratchian HP, Cross JB, Adamo C, Jaramillo J, Gomperts R, Stratmann RE, Yazyev O, Austin AJ, Cammi R, Pomelli C, Ochterski JW, Ayala PY, Morokuma K, Voth GA, Salvador P, Dannenberg JJ, Zakrzewski VG, Dapprich S, Daniels AD, Strain MC, Farkas O, Malick DK, Rabuck AD, Raghavachari K, Foresman JB, Ortiz JV, Cui Q, Baboul AG, Clifford S, Cioslowski J, Stefanov BB, Liu G, Liashenko A, Piskorz P, Komaromi I, Martin RL, Fox DJ, Keith T, Al-Laham MA, Peng CY, Nanayakkara A, Challacombe M, Gill PMW, Johnson B, Chen W, Wong MW, Gonzalez C, Pople JA (2009) Gaussian 09, revision C.01. Gaussian, Inc, Pittsburgh
65. Levine IN (2000) Quantum chemistry. Prentice-Hall, New Jersey
66. AIM2000 designed by Friedrich Biegler-König. University of Applied Sciences, Bielefeld, Germany
67. Bader RFW (1985) Acc Chem Res 18:9
68. Bader RFW (1991) Chem Rev 91:893
69. Bader RFW (1994) Atoms in molecules: a quantum theory. Oxford University Press, Oxford
70. Poater J, Solà M, Duran M, Fradera X (2002) Theor Chem Accounts 107:362
71. Firme CL, Antunes OAC, Esteves PM (2009) Chem Phys Lett 468:129
72. Bamfield P (2001) Chromic phenomena: the technological applications of colour chemistry. The Royal Society of Chemistry, Bristol
73. Sasirekha V, Umadevi M, Ramakrishnan V (2008) Spectrochim Acta A 69:148
74. Pinheiro JMF Jr, de Melo C (2011) J Phys Chem A 115:7994
75. Nadaf YF, Mulimani BG, Gopal M, Inamdar SR (2004) J Mol Struct (THEOCHEM) 678:177
76. Umadevi M, Vanelle P, Terme T, Ramakrishnan V (2006) J Fluoresc 16:569
77. Reichardt C, Welton T (2011) Solvents and solvents effects in organic chemistry, 4th edn. Wiley-VCH Verlag, Weinheim
78. Rezende MC, Dominguez M, Aracena A, Millan D (2011) Chem Phys Lett 514:267
79. Duan C, Huang F, Cao Y (2012) J Mater Chem 22:10416
80. Gong Y, Guo X, Wang S, Su H, Xia A, He Q, Bai F (2007) J Phys Chem A 111:5806

AUTHOR QUERIES

AUTHOR PLEASE ANSWER ALL QUERIES.

Q1. Please check captured table 1 footnote if correct.
Q2. Please provide article title for all journal articles.
Q3. Please provide complete bibliographic details for references 48, 49 and 66.
Q4. Please check Tables 1-3 if captured and presented correctly.